American Journal of Applied Chemistry
2023; 11(4): 103-111
http://www.sciencepublishinggroup.com/j/ajac
doi: 10.11648/j.ajac.20231104.12
ISSN: 2330-8753 (Print); ISSN: 2330-8745 (Online)

Electrochemical Detection of Paracetamol and Iohexol Using a Boron-Doped Diamond Anode Modified with Gold Particles

Koffi Konan Sylvestre[1, *], Kambiré Ollo[2], Gnamba Corneil Quand-même[1], Kimou Kouakou Jocelin[1], Berté Mohamed[1], Kouadio Kouakou Etienne[1], Koné Souleymane[1], Ouattara Lassiné[1, *]

[1]Matter Constitution and Reaction Laboratory, Training and Research Unit of Structural Sciences of Matter and Technology, Félix Houphouët-Boigny University, Abidjan, Côte d'Ivoire

[2]Science and Technology Training and Research Unit, University of Man, Man, Côte d'Ivoire

Email address:

syloekonan@gmail.com (Koffi Konan Sylvestre), ouatlassine@yahoo.fr (Ouattara Lassiné)

[*]Corresponding author

To cite this article:

Koffi Konan Sylvestre, Kambiré Ollo, Gnamba Corneil Quand-même, Kimou Kouakou Jocelin, Berté Mohamed, Kouadio Kouakou Etienne, Koné Souleymane, Ouattara Lassiné. Electrochemical Detection of Paracetamol and Iohexol Using a Boron-Doped Diamond Anode Modified with Gold Particles. *American Journal of Applied Chemistry*. Vol. 11, No. 4, 2023, pp. 103-111. doi: 10.11648/j.ajac.20231104.12

Received: July 8, 2023; **Accepted**: August 2, 2023; **Published**: August 28, 2023

Abstract: Persistent organic pollutants such as pharmaceuticals (iohexol and paracetamol) released into the environment is an environmental problem. Thus our objective is to propose an effective and less expensive method for the determination of their concentrations in the environment. In this work the detection and quantification of pharmaceuticals (iohexol and paracetamol) were performed using cyclic voltammetry and differential pulse voltammetry (DPV). The anode used is a boron-doped diamond electrode (BDD) modified with gold particles (Au-BDD). The characterization of the Au-BDD electrode surface by scanning electron microscopy coupled to energy dispersive spectroscopy and by the electrochemical method (cyclic voltammetry) showed the presence of gold particles uniformly distributed on the anode surface. DPV method allowed to obtain two calibration curves for iohexol and paracetamol concentrations ranging respectively from 4 µM to 67.42 µM and from 0.8 µM to 22.943 µM. The limits of detection are respectively 1.13 µM and 0.045 µM for iohexol and paracetamol. These results show that the presence of gold particles on the anode surface improved the detection of paracetamol. These pharmaceuticals were detected in an ionic environment and it was noted that the interference phenomenon was very negligible during the detection of these two pharmaceuticals. This shows that our anode can be used to determine PCM and IHX concentrations in highly charged media.

Keywords: Detection, Paracetamol, Iohexol, Gold, Voltammetry

1. Introduction

Emerging contaminants, such as pharmaceuticals, are a global problem for the last decades, as new pharmaceuticals are constantly being developed [1, 2]. Their enormous presence in the aquatic environment is mainly due to the disposal of industrial and especially pharmaceutical effluents, domestic and hospital wastewater [3-5]. Among these pharmaceutical products we have iohexol, iodinated contrast agents used on a large scale in radiology clinics, and medical imaging [6, 7]. Iohexol is a product whose molecule is non-biodegradable and non-transformable by the human body; it is eliminated entirely through the buttocks or urine once the medical diagnosis is completed [8]. In addition to iohexol, we have paracetamol which is frequently used to relieve pain, headaches and migraine. It is a drug widely used to reduce fever in children and adults. Its molecular structure is non-biodegradable so that it breaks down into very toxic metabolites [9]. The intensive use of paracetamol and iohexol in our hospitals and homes leads to their presence in the environment, and more precisely in surface water through the

sewage system. Their abundance in nature poses a real environmental problem especially for the living beings in our waters. The most commonly used techniques for the detection and quantification of these pharmaceuticals are capillary electrophoresis, liquid chromatography/mass spectrometry (LC/MS) [10, 11] and liquid chromatography (HPLC/UV) [12, 13]. All these approaches require sophisticated equipment and sufficient financial means. Therefore, the electrochemical detection of these pharmaceuticals is of interest. Several electrochemical sensors have demonstrated their performance in the detection and quantification of pharmaceuticals, including the platinum electrode [14], the carbon electrode [15], and the boron-doped diamond (BDD) [16]. BDD electrode is an electrode with a very high stability, chemical inertia, high thermal conductivity... [17, 18]. This electrode has been used as an electrochemical sensor for the detection of paracetamol (LOD = 0.47 µM) [9] and Iohexol (LOD = 1.953 µM) [19]. In order to improve the electrochemical properties of the BDD for the detection and quantification of paracetamol and iohexol, we will proceed to the modification of its surface by a transition metal like gold. In previous studies authors have shown that the modification of the electrode surface by gold nanoparticles would improve the electrochemical response due to the increase of the active surface and the intrinsic properties of gold at the nanometer size [20]. In this work we will use gold nanoparticle electrodeposition (three-pulse nucleation-growth deposition) on BDD to detect and quantify iohexol and paracetamol and then compare the results obtained by other researchers' research on these two pharmaceuticals.

2. Methods

2.1. Voltammetric Study

For the realization of this work an electrochemical cell comprising a working electrode, a reference electrode and a counter electrode was used. The working electrode is a boron doped diamond electrode modified by gold particles (Au-BDD). The counter electrode is a wound platinum wire and the reference electrode is a mercury sulfate electrode (MSE). Our three electrodes were connected to a PGSTAT 20 autolab (Ecochemie) connected by interface to a computer for data acquisition.

2.2. Chemicals

Potassium hydrogen phosphate hydrate ($K_2HPO_4.3H_2O$), sodium sulfate (Na_2SO_4) and magnesium Sulfate (Mg_2SO_4) was obtained from Merck. Sulfuric acid (H_2SO_4) was purchased from Panreac, Germany and $HAuCl_4$ (tetrachlorauric acid) solution was obtained from SIGMA-ALDRICH, USA. Iohexol (Omnipaque TM 300 mg I/mL, $C_{19}H_{26}I_3N_3O_9$) was provided by GE Healthcare (France) and paracetamol ($C_8H_9NO_2$) was purchased from a pharmacy in Abidjan. 1 mM stock solutions of paracetamol and iohexol were prepared separately by dissolving precise amounts of the drugs in an appropriate volume of 0.1 M H_2SO_4.

2.3. Pretreatment of the BDD

The BDD electrode underwent electrochemical pretreatment in a 0.5 M H_2SO_4 solution. For this pretreatment, an anodic pretreatment (+2 V, 15 s) is followed by a cathodic pretreatment (-2 V, 90 s). In this way, the BDD surface was first cleaned of all impurities and then rendered primarily hydrogen [9].

2.4. Deposition of Gold Particles

Electrochemical deposition of gold particles on BDD surface was performed in a 0.1 M H_2SO_4 solution containing 0.25 M $HAuCl_4$. We used three-pulse nucleation growth deposition (three-pulse deposition) [21, 22]. The potential and duration of the pulses induce rapid reduction of the gold avoiding significant hydrogen evolution and thus maintaining the surface termination of the electrode. A nucleation pulse consists of 2 s at -1.09 V/MSE, followed by growth pulses at -0.39 V/MSE (150 s, 300 s, 800 s respectively) [23]. After the three deposits, we rinsed the Au-BDD electrode with bidistilled water.

3. Results and Discussion

3.1. Characterization of the Synthesized Electrode Surface

3.1.1. Scanning Electron Microscopy

Figure 1A shows the scanning electron microscope (SEM) image of the boron-doped diamond electrode. In this image, randomly oriented crystals of a few micrometers in size with predominantly cubic and triangular faces can be distinguished. This image indicates that BDD has a polycrystalline structure [24, 25]. The grains are strongly bonded to each other. At the bottom of the diamond grains, a dark space is observed; this may be related probably to the graphitic carbon (Csp2) formed during the BDD preparation.

The image of the prepared Au-BDD electrode (Figure 1B) shows that its surface is coated with gold particles. These gold particles are uniformly distributed on BDD surface. However, at the bottom of the gold nanoparticles, the boron-doped diamond crystals are observed. This shows that our electrode is composed of boron-doped diamond crystals on which gold nanoparticles are attached.

Figures 1C and 1D show the scanning electron microscopies of carbon and gold of Au-BDD electrode, respectively. Figure 1C shows the presence of carbon particles on the surface of the new electrode, this presence of carbon observed would be due to the substrate (BDD) used to perform the electrodeposition of gold particles. From the observation of figure 1D, we can see that the gold nanoparticles obtained are well dispersed with a good coverage of the electrode surface. All this would attest that the gold electrodeposition followed by a progressive nucleation mechanism would promote a greater dispersion of gold nanoparticles and an increase in the amount of new nuclei for gold deposition on the BDD substrate.

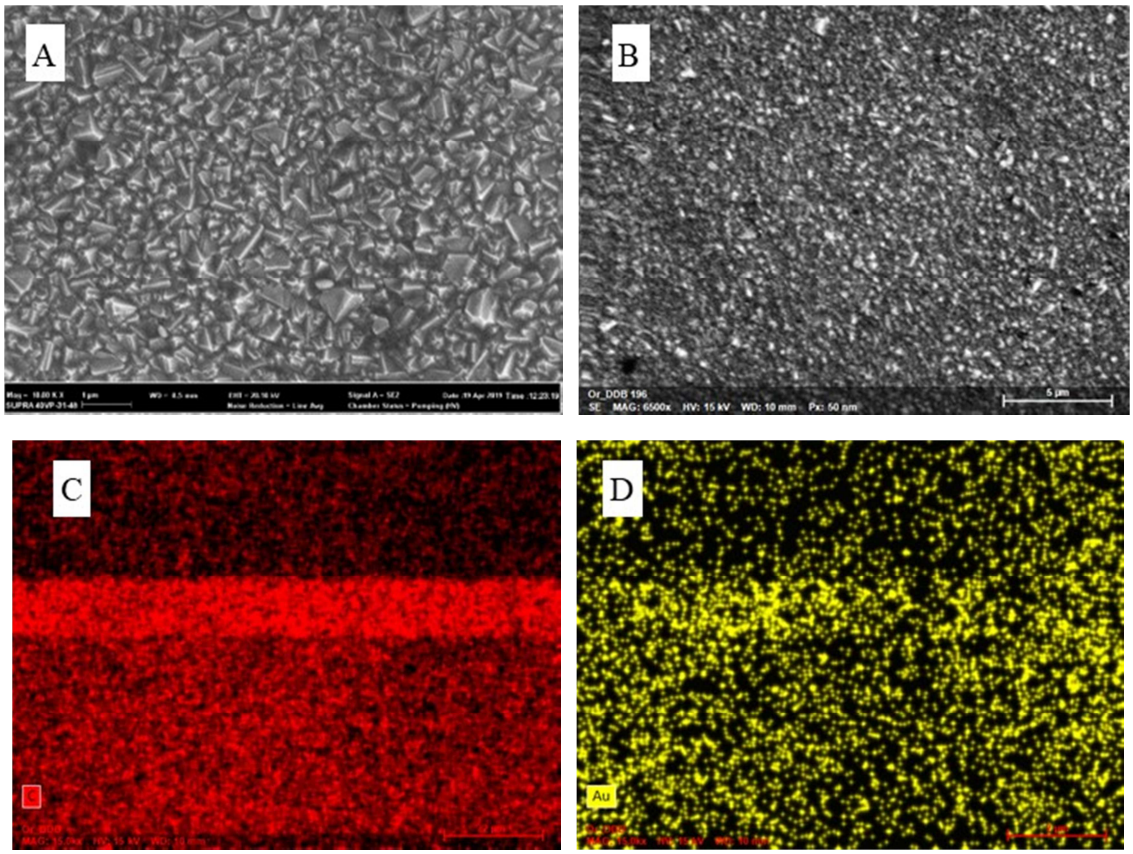

Figure 1. *SEM of BDD (A) and Au-BDD (B) surface, image of the carbon particles (C) and gold particles (D) of the Au-BDD electrode.*

3.1.2. Energy Dispersive Spectroscopy (EDS) Analysis

EDS measurements were performed on BDD and Au-BDD electrodes to determine the chemical composition of their surface. Figure 2 shows the EDS spectra obtained. The spectrum of the BDD electrode shows two intense peaks at 0.1 KeV and 1.9 KeV which characterize respectively the presence of carbon and silicon. We also note the presence of oxygen on electrode surface. Au-BDD spectrum shows peaks characteristic of carbon and silicon which were present on the BDD spectrum. Several peaks characteristic of gold are also observed on this spectrum. This shows that the Au-BDD electrode contains gold on its surface. These results confirm those obtained by SEM measurements. On the spectrum of the Au-BDD electrode, we note the presence of a characteristic peak of aluminum which would be due to a contamination of electrode surface during handling.

Table 1 shows the chemical elements present on the surface of the Au-BDD electrode and their mass percentage. This table confirms the presence of gold particles on the electrode surface. We also note the presence of Si which was present on the BDD electrode. It can be seen that the mass percentage of impurities due to Al is negligible (0.03%) compared to the other constituents.

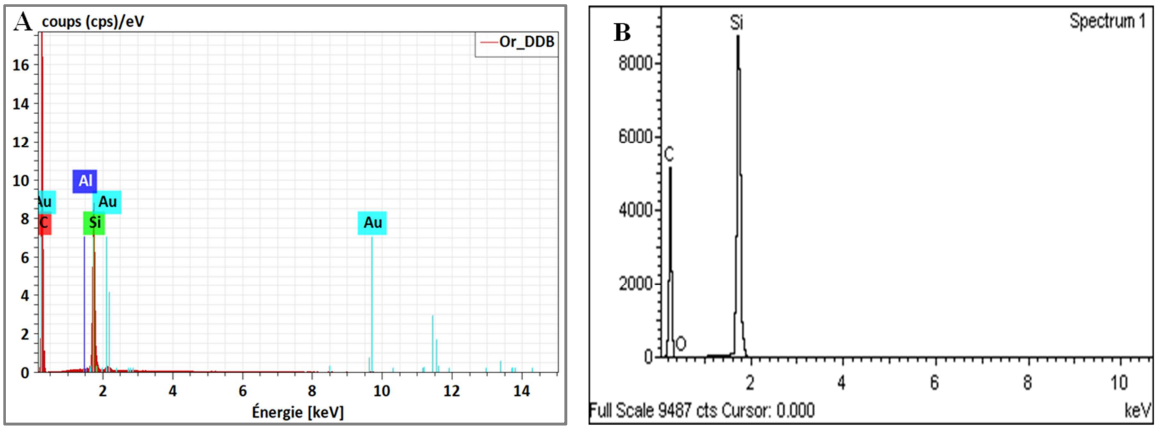

Figure 2. *EDS spectrum of BDD (A) and Au-BDD (B) electrodes.*

Table 1. *Mass percentage of chemical elements on Au-BDD electrode surface.*

Elements	C	Si	Au	Al	Total
Mass [%]	94.41	5.2	0.36	0.05	100

3.1.3. Electrochemical Characterization

Figure 3A shows the study performed on the behavior of the electrodes in potassium ferri-ferrocyanide solutions in the presence of potassium perchlorate (0.1 M) as supporting electrolyte. On this figure, the cyclic voltammograms of the two electrodes (Au-BDD and BDD) have the same appearance. On these voltammograms we observe that the intensities of the oxidation and reduction peaks are higher for Au-BDD and lower for BDD. This behavior of Au-BDD towards the ferri/potassium ferrocyanide couple indicates that the catalytic effect of the gold particles allowed the increase of the active surface.

Figure 3B shows the voltammograms of Au-BDD (red curve) and BDD (black curve) in sulfuric acid medium (0.1M). The measurement was performed at a scan rate of 20mV/s, in a potential range between 0 and 1 V/MSE. The curve representing the i = f (E) characteristic of the Au-BDD electrode shows peaks in both the forward and reverse directions of the potential scan, while that of the BDD shows no peaks in this chosen potential range. Indeed, in the forward direction, a peak is present at 0.729 V/MSE then the other at 0.886 V/MSE which would be related to the oxidation of the gold particles. There are two peaks in the return scan at 0.468 V/MSE and 0.335 V/MSE, reflecting the reduction of these gold oxides. These results confirm the presence of gold particles on the surface of our anode.

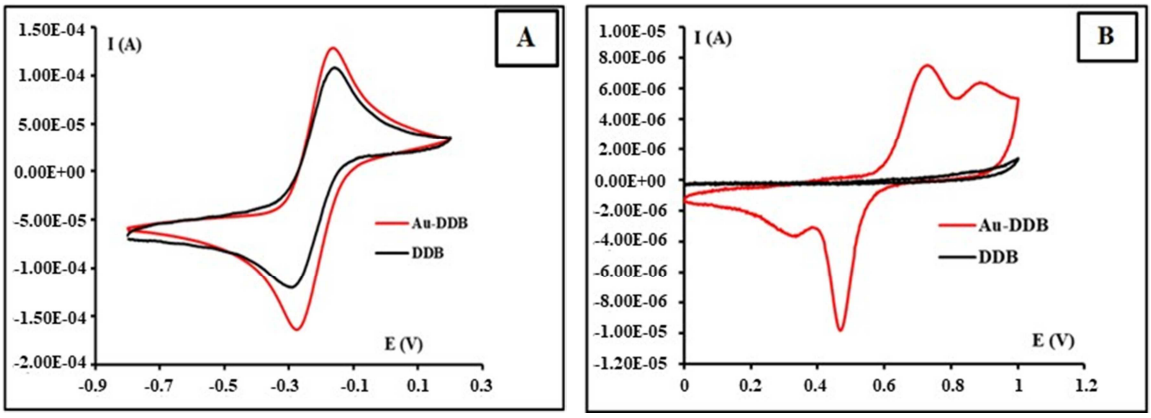

Figure 3. *(A) Cyclic voltammograms of* $Fe(CN)_6^{3-/4-}$ *on Au-BDD and BDD in* $KClO_4$*; (B) Cyclic voltammogram of Au-BDD and BDD in* H_2SO_4 *(0.1M).*

3.2. Voltammetric Measurements

3.2.1. Cyclic Voltammograms of Iohexol (IHX)

Figure 4A shows the voltammetric measurements in the presence of several concentrations of IHX (0.0625 mM to 1 mM) in H_2SO_4 (0.1 M). In this figure, we note that the oxidation peaks current intensity increases with increasing IHX concentration. The oxidation peak current intensity was studied as a function of IHX concentration. The curve obtained is straight with determination coefficient $R^2 = 0.9996$ (Figure 4B). The proportionality between peak current and IHX concentration shows that IHX is responsible for the observed peaks. The absence of peaks in the return direction would show an irreversible character of the phenomenon.

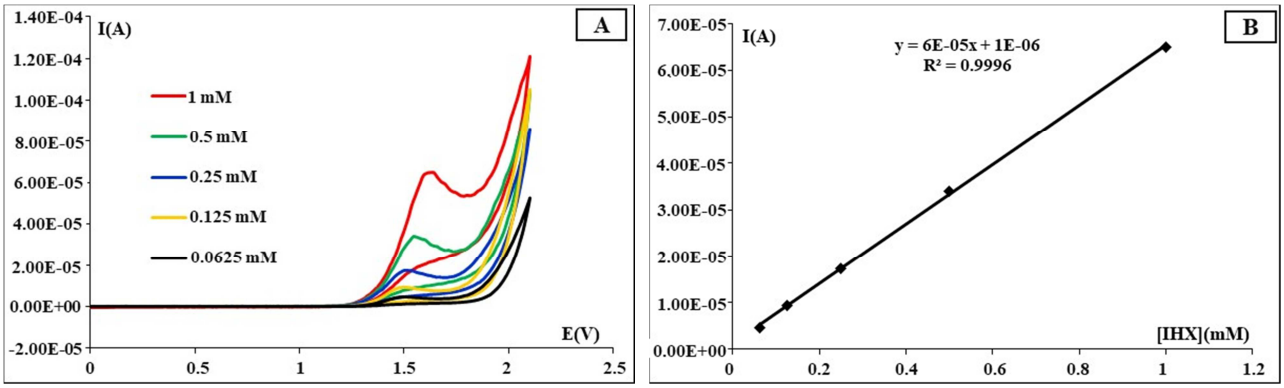

Figure 4. *(A) Cyclic voltammograms (CVs) of IHX in* H_2SO_4 *(0.1 M); (B):* J_P *curve as a function of Iohexol concentration. Scan rate: 50 mV/s.*

3.2.2. Cyclic Voltammograms of Paracetamol (PCM)

Figure 5A shows the CVs of our anode in the presence of various concentrations of PCM (0.125 mM to 2 mM) in H_2SO_4 (0.1 M). This figure shows that the value of the oxidation peaks potential increases with PCM concentration. It is also

noted that the peak current intensity increases with PCM concentration. Figure 5B shows that there is linearity between the oxidation peak current intensity and the concentration of drug product introduced into the reaction medium. The line obtained has a determination coefficient $R^2 = 0.9927$ which is very close to 1. This proves that the observed oxidation peak is related to the paracetamol.

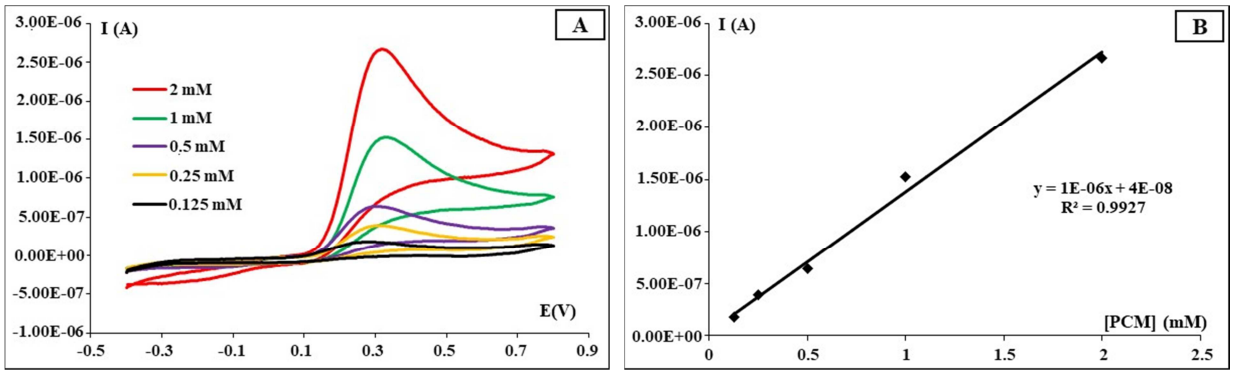

Figure 5. *(A) CVs of PCM in H_2SO_4 (0.1 M); (B): J_P curve as a function of paracetamol concentration; Scan rate: 50 mV/s.*

3.3. Differential Pulse Voltammetries

3.3.1. Measurement Conditions

To achieve better voltammetric detection of pharmaceuticals, we used the optimization conditions used by Koffi et al [26]. The optimization parameters used are listed in Table 2.

Table 2. *Measurement conditions for differential pulse voltammetries [26].*

Parameters	Iohexol
pretreatment potential (V)	-2
pretreatment time (s)	90
Modulation amplitude (V)	0.1
Modulation time (s)	0.05
Potential step (mV)	0.007

3.3.2. Differential Pulse Voltammetries of IHX

Au-BDD electrode was used to validate the method for detecting iohexol in sulfuric acid. The values of the IHX concentration chosen are between 0 µM and 67.42 µM. Figure 6 shows the results obtained. In this figure, an increase in the peak current density with IHX concentration of is noted.

The calibration curve was determined for IHX concentrations ranging from 4 µM to 67.42 µM. Over this concentration range, two lines with different slopes were obtained. The first curve obtained for concentrations starting from 4 µM to 15.81 µM is a straight line with determination coefficient of $R^2 = 0.9976$. In this range, the limit of detection (LOD) is 1.13 µM and limit of quantification (LOQ) is 3.78 µM. The limits of detection and limit of quantification were determined using the relationships (1) and (2). The second range of concentrations located between 23.53 µM and 67.42 µM made it possible to obtain a line of determination coefficient $R^2 = 0.9984$ which is very close to 1. This reflects a good linearity of the method for this range of concentration. For this chosen range the limit of detection is 2.56 µM and a LOQ of 8.54 µM. The limit of detection and the limit of quantification were determined using the relations (1) and (2).

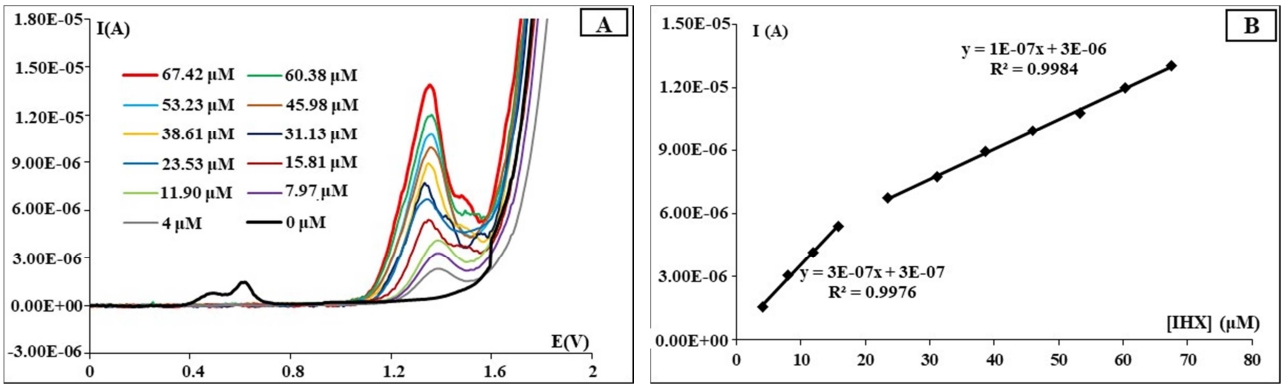

Figure 6. *(A) Differential pulse voltammetries (DPVs) of iohexol (0 µM to 67.42 µM) ; (B) J_P curve versus IHX concentration.*

$$LOD = 3*SD / b \quad (1)$$

$$LOQ = 10*SD / b \quad (2)$$

Where SD is the standard deviation of the current density signals and b is the slope of the method calibration curve.

3.3.3. Differential Pulse Voltammetries of PCM

Figure 7A shows differential pulse voltammeter curves recorded in sulfuric acid in the presence of PCM (0 µM to

22.943 µM). On this figure we notice that the oxidation peak of PCM evolves with the concentration introduced in the reaction media. The peak currents intensities of the various voltammograms obtained allowed to draw the calibration curve for the concentrations going from 0 µM to 22.943 µM (Figure 7B). The LOD and LOQ were calculated for this concentration range of PCM. The respective LOD and LOQ values are 0.045 µM and 0.133 µM.

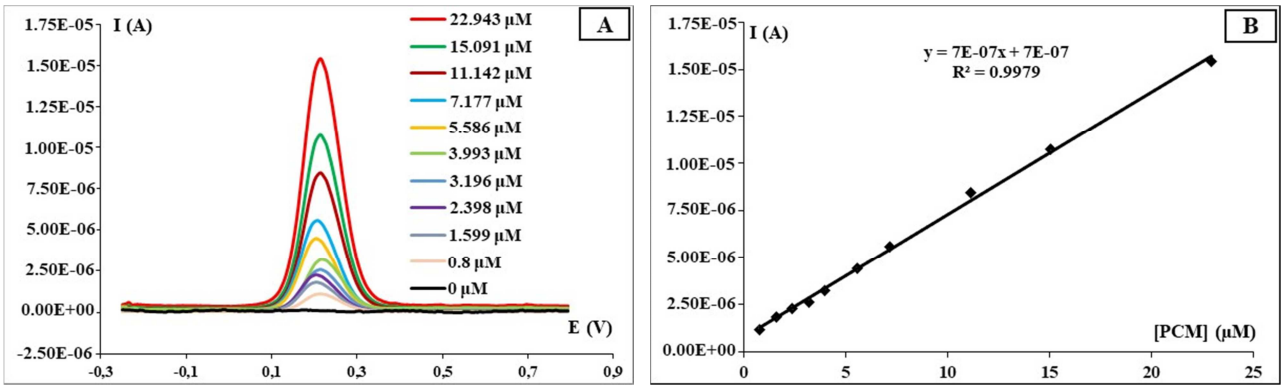

Figure 7. *(A) DPVs at different paracetamol concentrations (0 µM to 22.943 µM); (B) I_P curve as a function of PCM concentration.*

3.3.4. Influence of Inorganic Ions on IHX and PCM Detection

Inorganic ions exist in large quantities in the environment and can interfere with iohexol and paracetamol during its detection. The products we have chosen to study the phenomenon of interference are: di-potassium hydrogen phosphate hydrate ($2K^+$; HPO_4^{2-}), magnesium sulfate hydrate (Mg^{2+}; SO_4^{2-}) and sodium sulfate ($2Na^+$; SO_4^{2-}). This study occurred in a 0.1 M sulfuric acid solution containing IHX (20 µM) and PCM (20 µM). It should be noted that these studies were performed separately with respect to each drug product.

To these solutions of IHX and paracetamol, 3.846 mM; 7.407 mM and 10.714 mM were successively added which are the concentrations of the different products listed above. The peak current densities obtained by the DPV method in the presence of the interfering compounds were deduced from that obtained without interfering compounds. The formula for calculating the interference for each compound acting on the iohexol detection signal is:

$$X = \left(\frac{J'}{J} \times 100\right) - 100 \qquad (3)$$

Where J' is the peak density of the interfered signal of each drug product and J is that of the signal without interferents.

Table 3. *Influence of inorganic ions on IHX and PCM detection.*

Interfering Compounds	% change in peak current density in DPV (J - 100%) for IHX	% change in peak current density in DPV (J - 100%) for PCM
	-5.452	0.172
$K_2HPO_4.3H_2O$	-4.272	-5.122
	-1.971	-1.943
	4.067	-1.210
Na_2SO_4	-3.596	0.956
	-5.046	-4.121
	-1.390	0.804
Mg_2SO_4	-4.749	-2.723
	3.139	-5.057

Table 3 presented us the different values of interference. From the observation of this table we see that the percentage of interference is between ± 0.172 % and ± 5.452 % for the concentrations of K^+, HPO_4^{2-}, Mg^{2+}, SO_4^{2-}et Na^+ ions. It can be seen that the concentrations of these ions being more than 100 times higher than that of IHX and PCM produces a very negligible effect on the peak detection of these pharmaceuticals. This shows that these ions do not interfere with IHX and PCM detection. These results allow us to affirm that in an ion-laden environment such as wastewater, our method can be used for the detection and quantification of iohexol and paracetamol.

3.3.5. Comparison of IHX and PCM Detection Methods

Table 4 shows that our proposed analytical method is suitable for the detection and quantification of trace iohexol in wastewater, as the developed electrochemical sensor (Au-BDD) achieves a detection limit for trace iohexol (1.13 µM). This value is lower than the values found by some authors [19, 27-29]. This shows that the method is reliable.

Table 4. *Comparison of iohexol detection methods.*

Method	Media	Detection range	LOD	References
LC-MS/MS	Human serum	10 - 1000 µg/mL	3 µg/mL	[27]
CE (Capillary Electrophoresis	Human serum	13 - 305 mg/L	10 - 32 µg/mL	[28]
HPLC-UV	Rat Plasma	0.05 - 5 µg/mL		[29]
Electrochimic (DPV)	H_2SO_4 (0, 1M)	4 – 74.35 µM	1.953 µM	[19]
Electrochimic (DPV)	H_2SO_4 (0, 1M)	4 – 15.81 µM	1.13 µM	Present work

The comparison of our paracetamol detection method with literature methods is shown in Table 5. The table observation clearly indicates that our method is effective as it quantifies PCM with a LOD of 0.045 µM lower than literature values [9, 30-32].

Table 5. *Efficiency of the electrodes for the paracetamol detection by DPV.*

Electrode	Method	Detection range	LOD	References
AuNP-PGA/SWCNT	DPV	8.3 - 145.6	1.18	[30]
GR–CS/GCE	DPV	1-100	0.3	[31]
Graphite	DPV	5 -150	0.2	[32]
BDD	DPV	2.0-130.66	0.167	[9]
Au-BDD	DPV	0.8 – 22.943	0.045	Present work

4. Conclusion

The boron-doped Diamond electrode was modified with gold nanoparticles (Au-BDD). This prepared electrode was physically characterized by EDX couplet scanning electron microscopy and electrochemical method using cyclic voltammetry. These characterizations showed the presence of gold particles on BDD surface. Characterization in potassium ferri-ferrocyanide solutions indicates that the catalytic effect of the gold particles increased the electrode's active surface area. This new electrode was used in the development of an electroanalytical method, based on differential pulse voltammetry, for the detection and quantification of pharmaceuticals (iohexol and paracetamol) in synthetic wastewater. The method was selective for these two pharmaceuticals, when used in an environment loaded with ion and other pharmaceuticals. The precision of the voltammetric method used resulted in detection limits of 0.045 µM for paracetamol and 1.13 µM for iohexol. These results are significantly better than those obtained with the BDD anode. This shows that the presence of gold particles on the surface of the BDD anode improves the detection of pharmaceuticals. Without a gold particle on BDD, 0.47 µM and 1.953 µM were obtained for paracetamol and iohexol respectively. These pharmaceuticals were detected in an ionic environment and it was noted that the interference phenomenon was very negligible during the detection of these two pharmaceuticals. This shows that our anode can be used to determine PCM and IHX concentrations in highly charged media.

Acknowledgements

We greatly thank the Swiss National Funds for its financial support that allowed this work to be carried out. Our Team has received part of the grant IZ01Z0_146919 for that work. We also thank Prof. Bakayoko-Ly Ramata, prior the president of the University Felix Houphouet-Boigny for her help in the realization of that work.

References

[1] Sadia SP, Kambiré O, Gnamba CQ-M, Pohan LAG, Berté M, Ouattara L (2021) Mineralization of Wastewater from the Teaching Hospital of Treichville by a Combination of Biological Treatment and Advanced Oxidation Processes. Asian Journal of Chemical Sciences 10 (2): 1-10. DOI: 10.9734/AJOCS/2021/v10i219086

[2] Kimou KJ, Kambiré O, Koffi KS, Kouadio KE, Koné S, Ouattara L (2021) Electrooxidation of Iohexol in Its Commercial Formulation Omnipaque on Boron Doped Diamond Electrode. International Research Journal of Pure & Applied Chemistry 22 (11): 29-41. DOI: 10.9734/IRJPAC/2021/v22i1130444

[3] Yi X, Tran NH, Yin T, He Y, Gin KY-H (2017) Removal of selected PPCPs, EDCs, and antibiotic resistance genes in landfill leachate by a full-scale constructed wetlands system. Water Research 121: 46–60. doi: 10.1016/j.watres.2017.05.008.

[4] Le T-H, Ng C, Tran NH, Chen H, Yew-Hoong GK (2018) Removal of antibiotic residues, antibiotic resistant bacteria and antibiotic resistance genes in municipal wastewater by membrane bioreactor systems. Water Research 145: 498-508. https://doi.org/10.1016/j.watres.2018.08.060

[5] Rasheed T, Bilal M, Nabeel F, Adeel M, Iqbal HMN (2019) Environmentally-related contaminants of high concern: Potential sources and analytical modalities for detection, quantification, and treatment. Environment International 122: 52-66. https://doi.org/10.1016/j.envint.2018.11.038

[6] Mendoza A, Zonja B, Mastroianni N, Negreira N, López de Alda M, Pérez S, Barceló D, Gil A, Valcárcel Y (2016) Drugs of abuse, cytostatic drugs and iodinated contrast media in tap water from the Madrid region (central Spain): A case study to analyse their occurrence and human health risk characterization. Environment International 86: 107–118. doi: 10.1016/j.envint.2015.11.001

[7] Lopez-Prieto IJ, Wu S, Ji W, Daniels KD, Snyder SA (2020) A direct injection liquid chromatography tandem mass spectrometry method for the kinetic study on iodinated contrast media (ICMs) removal in natural water. Chemosphere 243: 125311. https://doi.org/10.1016/j.chemosphere.2019.125311

[8] Brillantino D, Ferro T, Brillantino C, Rossi E, Minelli R, Bignardi E, Tufano A, Zeccolini R, Zeccolini M (2020) Clinical pharmacology, use, and adverse reactions of intravenous iodinated contrast media in computed tomography. Journal of Radiology and Imaging 4 (1): 1-6 http://dx.doi.org/10.14312/2399-8172.2020-1

[9] Kouadio KE, Kambiré O, Koffi KS, Ouattara L (2021) Electrochemical oxidation of paracetamol on boron-doped diamond electrode: analytical performance and paracetamol degradation. J. Electrochem. Sci. Eng. 11 (2): 71-86; DOI: https://doi.org/10.5599/jese.932

[10] Denis MC, Venne K, Lesiège D, Francoeur M, Groleau S, Guay M, Cusson J, Furtos A (2008) Development and evaluation of a liquid chromatography-mass spectrometry assay and its application for the assessment of renal function. J Chromatogr A. 1189 (1-2): 410-416. doi: 10.1016/j.chroma.2007.12.061.

[11] Sirajuddin ARK, Afzal S, Muhammad IB, Abdul N, Sarfaraz M (2007) Simpler spectrophotometric assay of paracetamol in tablets and urine samples. Spectrochimica Acta Part A: Molecular and Biomolecular Spectroscopy 68 (3): 747-751. https://doi.org/10.1016/j.saa.2006.12.055

[12] Cavalier E, Rozet E, Dubois N, Charlier C, Hubert P, Chapelle JP, Krzesinski JM, Delanaye P (2008) Performance of iohexol determination in serum and urine by HPLC: validation, risk and uncertainty assessment. Clin Chim Acta. 396 (1-2): 80-85. doi: 10.1016/j.cca.2008.07.011.

[13] Weimeng S, Wu L, Zhen H, Yuehua Z, Qingli H, Mingzhu X (2014) Electrochemical sensing of acetaminophen based on poly (3, 4 ethylenedioxythiophene)/graphene oxide composites. Sensors and Actuators B: Chemical 193: 823-829. https://doi.org/10.1016/j.snb.2013.12.052

[14] Riham KA, Engy MS, Hussein MF, Rasha MEN (2021) Design and application of molecularly imprinted Polypyrrole/Platinum nanoparticles modified platinum sensor for the electrochemical detection of Vardenafil. Microchemical Journal 171: 106771. https://doi.org/10.1016/j.microc.2021.106771

[15] Geto A, Amare M, Tessema M, Admassie S (2012) Polymer-modified glassy carbon electrode for the electrochemical detection of quinine in human urine and pharmaceutical formulations. Anal Bioanal Chem. 404 (2): 525-30. doi: 10.1007/s00216-012-6171-8.

[16] Karine RT, Luciano CA, Pablo AM, Anne AM, Dilton MP, Diego PR, Anderson CO, Eduardo MR, Rodrigo AAM, Wallans TPDS (2020) Electrochemical detection of 3, 4-methylenedioxymethamphetamine (ecstasy) using a boron-doped diamond electrode with differential pulse voltammetry: Simple and fast screening method for application in forensic analysis. Microchemical Journal 157: 105088. https://doi.org/10.1016/j.microc.2020.105088

[17] Elizabeth AMG, Greg MS (2016) A comparison of boron-doped diamond thin-film and Hg-coated glassy carbon electrodes for anodic stripping voltammetric determination of heavy metal ions in aqueous media. Analytica Chimica Acta 575 (2): 180-189. https://doi.org/10.1016/j.aca.2006.05.094

[18] Koffi KS, Kambiré O, Kouadio KE, Kimou KJ, Ouattara L (2021) Detection of Lead (II) on a Boron-doped Diamond Electrode by Differential Pulse Anodic Stripping Voltammetry. Chemical Science International Journal 30 (7): 33-46. DOI: 10.9734/CSJI/2021/v30i730242

[19] Koffi KS, Foffié TAA, Kouadio KE, Kimou KJ, Kone S, Ouattara L (2021) Cyclic and differential pulse voltammetry investigations of an iodine contrast product using microelectrode of BDD. Mediterranean Journal of Chemistry 11 (3): 244-254. http://dx.doi.org/10.13171/mjc02109301594lassiné

[20] Saha K, Agasti SS, Kim C, Li X, Rotello VM (2012) Gold nanoparticles in chemical and biological sensing. Chem Rev. 112 (5): 2739-79. doi: 10.1021/cr2001178.

[21] Izquierdo J, Mizaikoff B, Kranz C (2016) Surface-enhanced infrared spectroscopy on boron-doped diamond modified with gold nanoparticles for spectroelectrochemical analysis. Phys. Status Solidi. 213 (8): 2056. https://doi.org/10.1002/pssa.201600222

[22] Kambiré O, Alloko KSP, Pohan LAG, Koffi KS, Ouattara L (2021) Electrooxidation of the Paracetamol on Boron Doped Diamond Anode Modified by Gold Particles. International Research Journal of Pure & Applied Chemistry 22 (4): 23-35. DOI: 10.9734/IRJPAC/2021/v22i430401

[23] Bottari F, Wael KD (2017) Electrodeposition of gold nanoparticles on boron doped diamond electrodes for the enhanced reduction of small organic molecules. Journal of Electroanalytical Chemistry 801: 521-526. https://doi.org/10.1016/j.jelechem.2017.07.053.

[24] Lévy-Clément C, Ndao NA, Katty A, Bernard M, Deneuville A, Comninellis C, Fujishima A (2003) Boron doped diamond electrodes for nitrate elimination in concentrated wastewater. Diamond and Related Materials 12 (3–7): 606-612. https://doi.org/10.1016/S0925-9635(02)00368-0.

[25] Kambiré O, Pohan LAG, Konan KF, Mohamed B, Gnamba CQ-M, Ouattara L (2002) Behavior of boron-doped diamond anode on methyl orange oxidation, J. Mater. Environ. Sci. 13 (11): 1264-1277.

[26] Koffi KM, Ouattara L (2019) Electroanalytical Investigation on Paracetamol on Boron-Doped Diamond Electrode by Voltammetry. American Journal of Analytical Chemistry 10: 562-578. doi.org/10.4236/ajac.2019.1011039.

[27] Faye BV, Gina KV, Fabiola C, Flavio G, Shannon H (2015) Determination of iohexol in human serum by a semi-automated liquid chromatography tandem mass spectrometry method. Clinical Biochemistry 48 (10–11): 679-685. https://doi.org/10.1016/j.clinbiochem.2015.03.017.

[28] Van HSK, Seaux L, Cavalier E, Speeckaert MM, Dumoulin E, Lecocq E, Delanghe JR (2016) Determination of iohexol and iothalamate in serum and urine by capillary electrophoresis. Electrophoresis 37 (17-18): 2363-7. doi: 10.1002/elps.201600084.

[29] Zhuang L, Gao J, Zeng Y, Yu F, Zhang B, Li M, Derendorf H, Liu C (2011) HPLC method validation for the quantification of lomustine to study pharmacokinetics of thermosensitive liposome-encapsulated lomustine containing iohexol for CT imaging in C6 glioma rats. Eur J Drug Metab Pharmacokinet 36 (2): 61-9. doi: 10.1007/s13318-011-0030-4.

[30] Minh-Phuong NB, Cheng AL, Kwi NH, Xuan-Hung P, Gi HS (2012) Determination of acetaminophen by electrochemical co-deposition of glutamic acid and gold nanoparticles. Sensors and Actuators B: Chemical 174: 318-324. https://doi.org/10.1016/j.snb.2012.08.012.

[31] Meixia Z, Feng G, Qingxiang W, Xili C, Shulian J, Lizhang H, Fei G (2013) Electrocatalytical oxidation and sensitive determination of acetaminophen on glassy carbon electrode modified with graphene–chitosan composite. Materials Science and Engineering: C 33 (3): 1514-1520. https://doi.org/10.1016/j.msec.2012.12.055.

[32] Margarita S, Roumen Z, Zdravka V, Velizar G, Claudia M, Benjamin V, Gergana K, Yana H, Lydia T-P (2023) The validity of using bare graphite electrode for the voltammetric determination of paracetamol and caffeine. International Journal of Electrochemical Science. 18 (5): 100120. https://doi.org/10.1016/j.ijoes.2023.100120